VOL. 9, NO. 8, AUGUST 2014 ISSN 1819-6608
ARPN Journal of Engineering and Applied Sciences


www.arpnjournals.com

TRANSIENT-RATE ANALYSIS FOR HYDRAULICALLY-FRACTURED GAS SHALE WELLS USING THE CONCEPT OF INDUCED PERMEABILITY FIELD

Freddy Humberto Escobar, Lina Marcela Montenegro and Karla María Bernal
Universidad Surcolombiana/CENIGAA, Avenida Pastrana - Cra 1, Neiva, Huila, Colombia
E-Mail: fescobar@usco.edu.co

ABSTRACT

Currently, the oil industry is focused on the exploitation of unconventional reservoirs. Wells in such unconventional resources as gas shale formations have to be hydraulically fractured for commercial production since the permeability is very low to ultralow reaching values in the order of nanodarcies. Also, gas shale wells are normally tested by recording the flow rate versus time readings under constant pressure conditions so an analysis of the reciprocal rate and reciprocal rate derivative following the *TDS* philosophy is presented for two cases in which the network of microfractures around the main fracture system provides an improvement of the permeability in such zone and one case in which the permeability is considered to be uniform. These three cases have been dealt in the literature with decline-curve analysis and the identification of the permeability model, dealt as a transition period, is conducted by type-curve matching which basically consists of a trial-and-error procedure. Here, we found that the application of the reciprocal rate derivative allows to easily identify the type of permeability model to be used: uniform, linear and exponential since the before-called transition period is shown on the derivative curve as a specific behavior which has been arbitrarily called "multilinear flow regime" displaying a slope of either 0.66 or 0.61 on the reciprocal rate derivative curve for the exponential and linear variation models, respectively. The extension of the *TDS* technique allows for the characterization of well test data so permeability, fracture length, skin factor and reservoir length are estimated and successfully verified by their application to synthetic and field examples.

Keywords: gas shale wells, transient-rate analysis, superposition, flow regimes, average reservoir pressure.

1. INTRODUCTION

The permanent search for finding new hydrocarbon resources is closely related to an appropriate reservoir characterization and management in which well test has played an important role. Nowadays, gas shale formations are the main target of several oil companies. Since gas shale permeability is ultralow, then, fracturing the formation is a common strategy for adequate hydrocarbon exploitation. Well test analyses conducted in several gas producing basins have revealed several flow behaviors as a function of the distance of the main fracture plane. Transition flow regimes have also been observed since the propagation radius of the pressure waves do not reach the reservoir boundaries. This implies that the evaluation of such parameters as reservoir length may be overestimated depending upon the flow regime used for the calculations.

It is normally expected in ultralow permeability formations that fracturing creates a main fracture plane and a network of microfractures around the well-fracture system. These microfractures may improve the average permeability of the reservoir in zones surrounding the fracture treatment as stated by Palmer, Moschovidis, and Cameron (2007), and Ge and Ghassemi (2011). Then, such models as those presented by Wattenbarger *et al*. (1998) and El-Banbi and Wattenbarger (1998) assume uniform permeability in the surroundings of the fracture system which may not be the proper case. Recently, Fuentes-Cruz, Gildin and Valko (2014) presented a mathematical model considering that the average effect of the failure of weak planes leads to a non-uniform permeability distribution depending on the distance to the hydraulic fracture which becomes the basis of this work. They performed reservoir characterization by using rate-decline analysis which here is extended to transient rate analysis using the reciprocal rate and the reciprocal rate derivative by following the *TDS* philosophy, Tiab (1993).

In their work, Fuentes-Cruz *et al*. (2014) modeled three cases of permeability variation: uniform (with no variation in permeability), linear and exponential. They used type-curve matching for the identification of the appropriate permeability model type which is dealt in a very different and more practical form in this work. It was found that, as expected, the uniform model has no permeability variations then the linear flow is followed by the pseudosteady-state regime. However, for the linear and exponential models, Fuentes-Cruz *et al*. (2014) reported a transition period between linear flow regime and pseudosteady regime which we have found to be a possible flow regime, called arbitrarily here as multilinear, which is reflected as a slope of 0.66 and 0.61 on the reciprocal rate derivative curve for exponential and linear models, respectively. The proposed methodology is useful to estimate permeability, fracture length, reservoir length and skin factor. Also, geometrical skin factors for the above-named multilinear flows were introduced. The proposed technique was successfully tested with synthetic and field cases.

The superposition function is customary employed in analyzing rate tests conducted in gas shale formations. However, the tendency is to use the radial superposition function for all the flow regimes. Escobar,

Alzate and Collazos (2013) presented an analysis for such flow regimes as bilinear, linear, elliptical and pseudosteady and determined to use each function separately.

The application of transient-rate analysis using the reciprocal rate derivative has been recently used by Escobar, Sanchez and Cantillo (2008) in homogeneous and heterogeneous gas reservoirs, Escobar, Rojas, and Bonilla (2012) for elongated homogeneous and heterogeneous formations and Escobar, Castro and Mosquera (2014) for hydraulically fractured vertical hydrocarbon wells in conventional reservoirs. They applied the *TDS* technique in their studies. A recent application of the straight-line conventional analysis was also presented by Escobar, Rojas, and Cantillo (2012) for long homogeneous and naturally fractured formations.

2. MATHEMATICAL FORMULATION

2.1. Mathematical model

This study, initially presented by Montenegro-G. and Bernal-V. (2014), is based upon the mathematical model introduced by Cruz-Fuentes *et al*. (2014) as given below:

The dimensionless Laplacian pressure solution for permeability field is:

$$\bar{P}_D = \frac{\delta\pi}{u\sqrt{u}}\left[\frac{I_1\left(\frac{2y_D^*\sqrt{u}}{\ln(\xi)}\right)K_0\left(\frac{2y_D^*}{\ln(\xi)}\sqrt{\frac{u}{k_D^*}}\right)+I_0\left(\frac{2y_D^*}{\ln(\xi)}\sqrt{\frac{u}{k_D^*}}\right)K_1\left(\frac{2y_D^*\sqrt{u}}{\ln(\xi)}\right)}{I_0\left(\frac{2y_D^*\sqrt{u}}{\ln(\xi)}\right)K_0\left(\frac{2y_D^*}{\ln(\xi)}\sqrt{\frac{u}{k_D^*}}\right)-I_0\left(\frac{2y_D^*}{\ln(\xi)}\sqrt{\frac{u}{k_D^*}}\right)K_0\left(\frac{2y_D^*\sqrt{u}}{\ln(\xi)}\right)}\right] \quad (1)$$

(If k_D^*<1, δ=-1 and ξ=1/ k_D^*; if k_D^*>1, δ=1 and ξ= k_D^*)

The solution for the linear permeability case is:

$$\bar{P}_D = \frac{\delta\pi}{u\sqrt{u}}\left[\frac{I_1\left(\frac{2y_D^*\sqrt{k_D^*u}}{|K^*_D-1|}\right)K_0\left(\frac{2y_D^*\sqrt{u}}{|K^*_D-1|}\right)+I_0\left(\frac{2y_D^*\sqrt{u}}{|K^*_D-1|}\right)K_1\left(\frac{2y_D^*\sqrt{k_D^*u}}{|K^*_D-1|}\right)}{I_1\left(\frac{2y_D^*\sqrt{k_D^*u}}{|k_D^*-1|}\right)K_1\left(\frac{2y_D^*\sqrt{u}}{|k_D^*-1|}\right)-I_1\left(\frac{2y_D^*\sqrt{u}}{|k_D^*-1|}\right)K_1\left(\frac{2y_D^*\sqrt{k_D^*u}}{|k_D^*-1|}\right)}\right] \quad (2)$$

(If k_D^*<1, δ=-1; k_D^*>1, δ=1)

For uniform permeability ($k_D^*=1$):

$$\bar{P}_D = \frac{\pi}{u\sqrt{u}}\coth\left(y_D^*\sqrt{u}\right) \quad (3)$$

The dimensionless production rate is:

$$\bar{q}_D = \frac{1}{u^2\bar{P}_D} \quad (4)$$

The dimensionless time for oil and gas wells in field units is,

$$t_D = \frac{0.0002637k^0t}{\phi(\mu c_t)_i x_e^2} \quad (5)$$

The dimensional length stimulated reservoir volume.

$$y_D = \frac{y}{x_e} \quad (6)$$

The dimensionless permeability quantities for exponential and linear cases, respectively, are,

$$k_D(y_D) = \frac{k(y)}{k^0} = k_D^{*(y_D/y_D^*)} = e^{(\ln k_D^*)^{*(y_D/y_D^*)}} \quad (7)$$

$$k_D(y_D) = \frac{k(y)}{k^0} = 1+(k_D^*-1)\left(y_D/y_D^*\right) \quad (8)$$

The dimensionless minimum permeability is given also as,

$$k_D^* = \frac{k^*}{k^0} \quad (9)$$

The dimensionless gas flow reciprocal rate and reciprocal rate derivative, respectively, are:

$$\frac{1}{q_D} = \frac{n_f k^0 h\left[m(P_i)-m(P_{wf})\right]}{1424T}\frac{1}{q_g} \quad (10)$$

$$\left[t_D*(1/q_D)'\right] = \frac{n_f kh\left[\Delta m(P)\right]}{1424T}\left[t*(1/q)'\right] \quad (11)$$

The dimensionless oil flow reciprocal rate and reciprocal rate derivative, respectively, are:

$$\frac{1}{q_D} = \frac{n_f k^0 h(P_i-P_{wf})}{141.2B\mu}\frac{1}{q_0} \quad (12)$$

$$t_D*(1/q)'_D = \frac{kh\left(P_i-P_{wf}\right)}{141.2\mu B}\left(t*(1/q)'\right) \quad (13)$$

Using the concept of stimulated reservoir volume, the length of the hydraulic fracture ($2x_f$) is equal to the lateral extent of the volume that is stimulated, Fuentes-Cruz *et al*. (2014):

$$2x_f = x_e \quad (14)$$

2.2. TDS formulation for linear flow regime

This flow regime is presented in the three dealt models: uniform, linear and exponential. It is characterized

by a typical 0.5-slope line on the reciprocal rate derivative curve. As expressed by Fuentes-Cruz *et al*. (2014) at short times is governed by the following equation:

$$\frac{1}{q_D} = \pi^{\frac{3}{2}}\sqrt{t_D} \tag{15}$$

This flow regime takes place at about the same period of time for the different y_D as shown in Figures-1 through 3. Therefore, its behavior does not depend upon neither the variation of the dimensionless reservoir length nor the minimum permeability value.

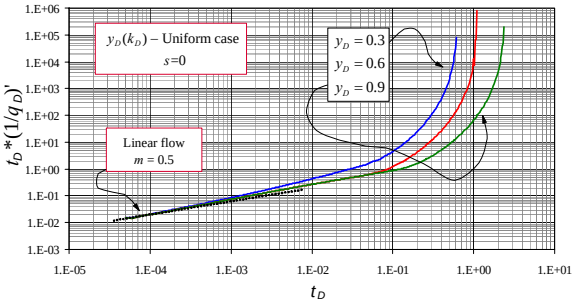

Figure-1. Effect of the dimensionless reservoir length (y_D^*) on the flow behavior for the uniform linear case, (k_D^*=0.15).

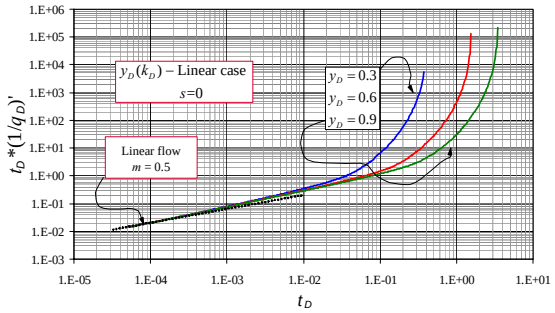

Figure-2. Effect of the dimensionless reservoir length (y_D^*) on the flow behavior for the linear flow, (k_D*=0.1)

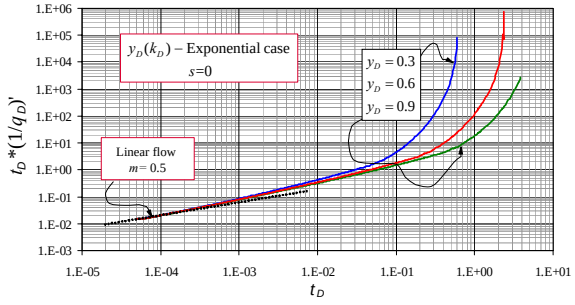

Figure-3. Effect of the dimensionless reservoir length (y_D^*) on the flow behavior for the exponential case, (k_D^*=0.1).

Once the dimensionless quantities given by Equations (5) and (10) are replaced into Equation (15), and taking the derivative to Equation (15) and, also, replacing in it the dimensionless quantities, it yields, respectively,

$$\frac{1}{q_{g\ L}} = \frac{128.76T\sqrt{t_L}}{n_f h\left[m(P_i)-m(P_{wf})\right]x_e(k^0\phi\mu c_t)^{1/2}} \tag{16}$$

$$t*(1/q_g)'_L = \frac{64.38T\sqrt{t_L}}{n_f h\left[m(P_i)-m(P_{wf})\right]x_e(k^0\phi\mu c_t)^{1/2}} \tag{17}$$

Since linear flow is independent of the minimum permeability -at the end of the main plane of fracture- Equations (16) and (17) allow to obtain respective expressions for obtaining the maximum induced permeability, k^0, by reading the values of reciprocal rate and reciprocal rate derivative at any arbitrary time during linear flow regime, so that:

$$k^0 = \frac{16579.82t_L}{\phi\mu c_t}\left\{\frac{T}{n_f h\left[m(P_i)-m(P_{wf})\right]x_e(1/q_g)_L}\right\}^2 \tag{18}$$

$$k^0 = \frac{4144.95t_L}{\phi\mu c_t}\left\{\frac{T}{n_f h\left[m(P_i)-m(P_{wf})\right]x_e[t*(1/q_g)'_L]}\right\}^2 \tag{19}$$

Notice that the reservoir length, x_e, can be solved from Equation (19),

$$x_e = \frac{64.38T\sqrt{t_L}}{n_f h\left[m(P_i)-m(P_{wf})\right][t*(1/q_g)'_L](k^0\phi\mu c_t)^{1/2}} \tag{20}$$

Fuentes-Cruz *et al*. (2014) introduce an expression to estimate skin factor from a point on the reciprocal rate curve during linear flow regime. That expression is rewritten here as:

$$s_{initial} = \frac{n_f k^0 h\left[m(P_i)-m(P_{wf})\right]}{1424T}\left(\frac{1}{q_g}\right)_L \tag{21}$$

2.3. *TDS* Formulation for multilinear flow regime

For both linear and exponential permeability distribution models, Fuentes-Cruz *et al*. (2014) point out the existence of a transition period between the linear flow regime and the boundary-dominated pseudosteady state (BDS). However, we have found that such transitions may behave as a new flow regime since the reci [procal rate derivative reflects very characteristic new slopes which are not reported in the literature. We assume that this flow regime may result from a combination of several flow regimes, then, we have arbitrarily call that as "*multilinear flow regime*". However, we recommend conducting a simulation in order to properly identify the streamlines

acting in such case and, then, identify and name the observed flow regime.

For the case of the linear permeability model, the multilinear flow is defined by a slope of 0.61 on a log-log plot of the reciprocal rate derivative. As seen in Figure-5, the flow behavior is independent of the variation in the dimensionless permeability (k_D), then its representative equation developed in this work is given below,

$$t_D*(1/q_D)'_{MLL}=\frac{250}{50}(t_D)^{0.6135}_{MLL} \quad (22)$$

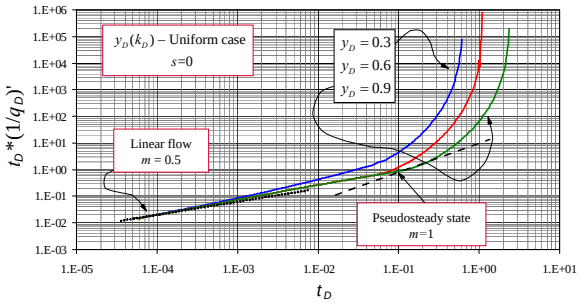

Figura-4. Absence of multilinear case for uniform flow, with effects of variation of permeability in the stimulated reservoir volume (k_D^*) at constant y_D.

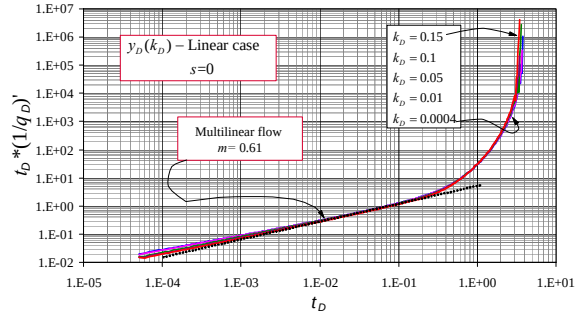

Figure-5. Multilinear flow behavior during the linear model with different permeability values (k_D^*) and constant y_D.

Suffix *MLL*, in Equation (22), stands for *Multilinear Flow* in the linear permeability model. After, replacing the dimensionless terms given by Equations (5) and (11) into Equation (22), expressions to estimate either permeability or reservoir length from Equation (22) are obtained:

$$k_{MLL}=\left\{\frac{44.380384T(t)^{0.6135}}{(\phi\mu c_{ti})^{0.6135}x_e^{1.227}n_f h\left[m(P_i)-m(P_{wf})\right]\left[t*(1/q)'_{MLL}\right]}\right\}^{\frac{1}{0.3865}} \quad (23)$$

$$x_e=\left\{\frac{44.380384T(t)^{0.6135}}{(\phi\mu c_{ti})^{0.6135}k^{0.3865}n_f h\left[m(P_i)-m(P_{wf})\right]\left[t*(1/q)'_{MLL}\right]}\right\}^{\frac{1}{1.227}} \quad (24)$$

Notice that the permeability value obtained from Equation (23) does not correspond to the initial permeability value, k^0, since the permeability value is going under a decay process related to the distance from the fracture system.

Once the lateral reservoir length is estimated, the fracture length, x_f, is calculated with Equation (14) in which Fuentes-Cruz et al. (2014) pointed out that lateral extension of the stimulated reservoir volume is two fold the hydraulic fracture length, x_e, then ($2x_f = x_e$), considering a rectangular geometry reservoir.

Following the philosophy of the *TDS* technique, the geometrical skin factor, s_{MLL}, occurring due to the change from linear to multilinear flow regimes is obtained by taking the ratio between the reciprocal rate –integration of Equation (22) and the reciprocal rate derivative given by Equation (22), then solving for s_{MLL}:

$$s_{MLL}=0.03117\left(\frac{kt_{MLL}}{\phi\mu c_t x_e^{\,2}}\right)^{0.6135}\left[\frac{(1/q)_{MLL}}{t*(1/q)'_{MLL}}+1.629991\right] \quad (25)$$

For the case of the linear permeability model, the multilinear flow for the case of the exponential permeability model is defined by a slope of 0.66 on a log-log plot of the reciprocal rate derivative. It gives a relationship of three log cycles in the time axis against two log cycles in the reciprocal rate derivative axis. As shown in Figure-6, the flow behavior does not present a uniformity related to the variation of k_D, then, it was necessary to determine the most representative mathematical representation of the multilinear flow behavior which was performed by using a probabilistic average,

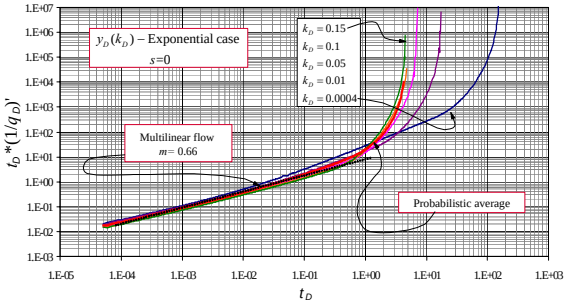

Figure-6. Multilinear flow behavior during the exponential model with different permeability values (k_D^*) and constant y_D.

$$t_D*(1/q_D)'_{MLE}=\frac{405}{50}(t_D)^{0.6612}_{MLE} \quad (26)$$

Once again, after plugging the dimensionless terms in Equation (26), expressions for either permeability and reservoir length can be obtained, such as,

$$k_{MLL}=\left\{\frac{49.66812320T(t)^{0.6612}}{(\phi\mu c_{ti}x)^{0.6612}x_e^{1.3224}n_f h\left[m(P_i)-m(P_{wf})\right]\left[t*(1/q)'_{MLL}\right]}\right\}^{\frac{1}{0.3388}} \quad (27)$$

$$x_e=\left\{\frac{49.66812320T(t)^{0.6612}}{(\phi\mu c_{ti}x)^{0.6612}k^{0.3388}n_f h\left[m(P_i)-m(P_{wf})\right]\left[t*(1/q)'_{MLL}\right]}\right\}^{\frac{1}{1.3224}} \quad (28)$$

As for the linear permeability model, the geometrical skin factor, s_{MLE}, is obtained by the dividing the reciprocal rate equation resulting from the integration of Equation (26) and the reciprocal rate derivative, Equation (26), and solving for the skin factor, so:

$$s_{MLE}=0.03488\left(\frac{kt_{MLE}}{\phi\mu c_t x_e^{\,2}}\right)^{0.6612}\left[\frac{(1/q)_{MLE}}{t*(1/q)'_{MLE}}-1.512402\right] \quad (29)$$

2.4. *TDS* formulation for Pseudosteady-state regime

The determination of the governing equation for the late pseudosteady period requires a log-log plot of $t_D*(1/q_D)'$ versus t_{DA} using a dimensionless constant permeability (k_D = constant) and different dimensionless length values (y_D = 0.3, 0.6 and 0.9), for each one of the induced permeability models. In each model, a uniform behavior was found by dividing the dimensionless time by the dimensionless length of the stimulated volume reservoir for each case respectively,

$$t_{DA}=\frac{t_D}{y_D^2} \quad (30)$$

Similarly to transient-pressure analysis, the late pseudosteady-state regime is used for the calculation of the well drainage area without using the permeability value. Needless to say that the in transient-rate analysis the derivative during pseudosteady state does not follow to a unit-slope line, but a constantly increasing curve instead, then, a tangent unit-slope line must be drawn on the derivative curve during this late time for the characterization of such regime, See Figures-7, 8 and 9.

For the uniform model, Figure-7, the dimensionless reciprocal rate derivative governing equation during pseudosteady-state regime is given below,

$$\frac{\left[t*(1/q_D)'\right]_{PSSU}}{y_D}=\frac{57}{25}\pi\left(\frac{t_D}{y_D^2}\right)_{PSSU} \quad (31)$$

After the dimensionless terms given by Equations (5), (6) and (11) are replaced in Equation (31), an expression for the determination of the lateral reservoir length, x_e, is obtained,

$$x_e=\frac{\frac{57}{25}\pi(0.0002637)(1424)T}{n_f\phi h(\mu c_t)_i y\left[m(P_i)-m(P_{pwf})\right]}\frac{t_{PSSU}}{\left[t*(1/q)'\right]_{PSSU}} \quad (32)$$

For the linear model, Figure-8, the dimensionless reciprocal rate derivative governing equation during pseudosteady-state regime is given as follows,

$$\frac{\left[t*(1/q_D)'\right]_{PSSL}}{y_D}=\frac{153}{50}\pi\left(t_{DA}\right)_{PSSL} \quad (33)$$

From which an expression to estimate the lateral reservoir length is developed once the dimensionless parameters are replaced in Equation (33),

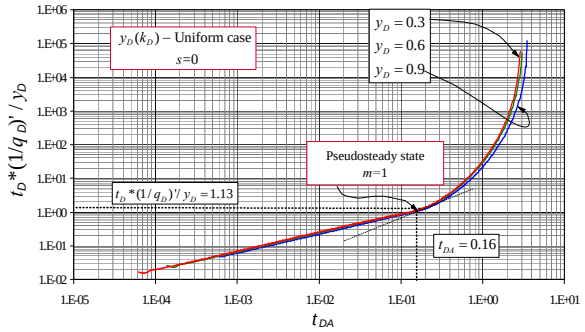

Figure-7. Effect of the variation of the dimensionless length on the pseudosteady state regime for the uniform model with k_D constant.

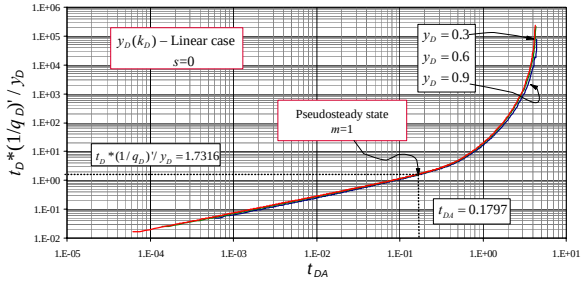

Figure-8. Pseudosteady state behavior on the linear model with constant k_D and the effect of varying the length of field stimulated.

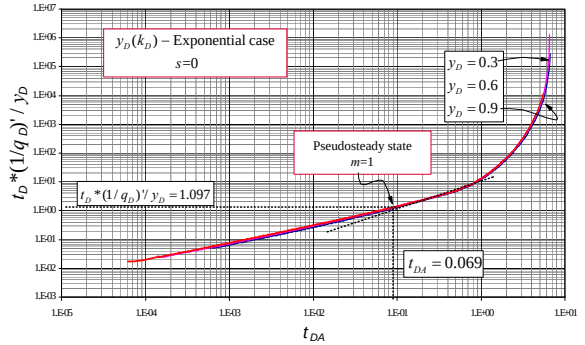

Figure-9. Effect of varying the reservoir length in the exponential model with constant k_D.

$$x_e = \frac{\frac{153}{100}\pi * 0.0002637 * 1424 * T}{n_f h \phi (\mu c_t)_i y\left[m(P_i) - m(P_{pwf})\right]} \frac{t_{PSSL}}{\left[t*(1/q)'\right]_{PSSL}} \quad (34)$$

For the exponential permeability model, Figure-9, the reciprocal rate derivative governing equation in dimensionless form which takes place during pseudosteady-state regime is shown as,

$$\frac{\left[t_D*(1/q_D)'\right]_{PSSE}}{y_D} = \frac{101}{20}\pi\left(\frac{t_D}{y_D^2}\right)_{PSSE} \quad (35)$$

Which also leads to the development of an equation to find reservoir length after the replacement of the dimensionless time, Equation (5), and the dimensionless reciprocal rate derivative, Equation (11),

$$x_e = \frac{\frac{101}{20}\pi * 0.0002637 * 1424 * T}{n_f h \phi (\mu c_t)_i y\left[m(P_i) - m(P_{pwf})\right]} \frac{t_{PSSE}}{\left[t*(1/q)'\right]_{PSSE}} \quad (36)$$

Finally, it is possible to write a general dimensionless derivative equation for the pseudosteady state period,

$$\frac{\left[t*(1/q_D)'\right]}{y_D} = \alpha\pi\left(t_{DA}\right) \quad (37)$$

The value of α is reported in Table-1 depending on the permeability model.

Table-1. Values of alpha for the general dimensionless derivative equation for the pseudosteady state period.

Model	α
Exponential	101/20
Linear	153/100
Uniform	57/25

2.5. Intersection points of the uniform model

The intersection point formed by the drawn line on the linear flow regime given by derivative of Equation (15) with the psuedosteady state period line, t_{LPSSUi}, is provided below as,

$$\left(\frac{0.0002637 k^* t_{LPSSUi}}{\phi(\mu c_t)_i}\right)^{0.5} = 0.388 y \quad (38)$$

Equation (38) allows to solve for the maximum induced permeability,

$$k^\circ = \left[\frac{23.9225 y\left[\phi(\mu c_t)_i\right]^{0.5}}{t_{LPSSU_i}^{0.5}}\right]^2 \quad (39)$$

2.6. Intersection points of the linear model

At the point, t_{LPSSLi}, at which the psudosteady-state period, Equation (33) intersects with the linear flow regime given by Equation (15), is given below,

$$\left(\frac{0.0002637 k^0 t_{LPSSLi}}{\phi(\mu c_t)_i}\right)^{0.5} = 0.28905 y \quad (40)$$

The maximum permeability value can be solved from the above equation to give,

$$k^0 = \left[\frac{17.7999 y\left[\phi(\mu c_t)_i\right]^{0.5}}{t_{LPSSL_i}^{0.5}}\right]^2 \quad (41)$$

The point of intersection, $t_{MLPSSLi}$, between the late pseudosteady state regime, Equation (33), and the multilinear flow regime, Equation (22), gives the following equation in dimensional terms:

$$\left(\frac{0.0002637 k^* t_{MLPSSL_i}}{\phi(\mu c_t)_i x_e^2}\right)^{0.3865} = 0.5077\frac{y}{x_e} \quad (42)$$

This allows to solve for the low permeability induced in dimensional terms (k^*),

$$k^* = \left[12.27\frac{y}{x_e^{0.227}}\left(\frac{\phi(\mu c_t)_i}{t_{MLPSSL_i}}\right)^{0.3865}\right]^{1/0.3865} \quad (43)$$

2.7. Intersection points of the exponential model

The intersection point of the pseudosteady state [Equation (35)] and linear flow regime given by the derivative of Equation (15), t_{LPSSEi}, provides the following expression,

$$\left(\frac{0.0002637 k^0 t_{LPSSEi}}{\phi(\mu c_t)_i}\right)^{0.5} = 0.1755 y \quad (44)$$

Equation (45) is useful to recalculate the maximum induced permeability,

$$k^0 = \left[\frac{10.8074 y\left[\phi(\mu c_t)_i\right]^{0.5}}{t_{LPSSE_i}^{0.5}}\right]^2 \quad (45)$$

The intersection point formed between the pseudosteady state regime, Equation (37), and the multilinear flow regimen given by Equation (26), $t_{MLPSSEi}$, provides the following equation,

$$\left(\frac{0.0002637 k^* t_{MLPSSL_i}}{\phi(\mu c_t)_i x_e^2}\right)^{0.3388} = 0.5111\frac{y}{x_e} \quad (46)$$

Which is also useful to develop an expression for the estimation of the minimum induced permeability,

$$k^* = \left[8.3375 \frac{y}{x_e^{0.3224}} \left(\frac{\phi(\mu c_t)_i}{t_{MLPSSE_i}} \right)^{0.3388} \right]^{1/0.3388} \quad (47)$$

Table-2. Relevant information for each model.

Parameter	Value	Parameter	Value
h (ft)	400	μ_g (cp)	0.018
ϕ (%)	5.2	x_e (ft)	600
T (°R)	633.5	P_i (psi)	3115
B_{gi} (rb/Mscf)	0.916	P_{wf} (psi)	500
$m(P_i)$ (psi^2/cp)	5.15x108	c_t (psi^{-1})	1.85x10^{-4}
$m(P_{wf})$ (psi^2/cp)	2.08x107	y (ft)	300
k (md)	0.05	n_f	2
s	0		

4. EXAMPLES

Three synthetic and one field examples are worked for the applicability of the above-developed equations for each model. Table-2 provides relevant information of the reservoir, well and fluid properties employed in each one of the permeability models.

4.1. Example-1: Uniform model

For the case under consideration, the reciprocal rate and its derivative are reported in Figure-10 with the purpose of determining the permeability, fracture length and reservoir length.

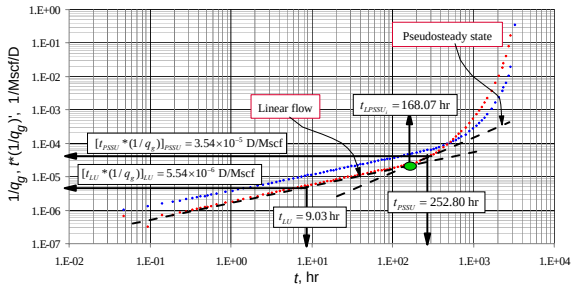

Figure-10. Log-log plot of the reciprocal rate and the reciprocal rate derivative vs. time for the uniform synthetic example.

Solution. As expected for this example, only linear flow regime and pseudosteady state period are developed. The below parameters were read from Figure-11.

$(t)_{LU}$ = 9.030 hr
$(1/q_g)_{LU}$ = 1.1134x10^{-5} day/Mscf
$[t *(1/q_g)']_{LU}$ = 5.5375x10^{-6} day/Mscf
$(t)_{PSSU}$ = 252.8018 hr
$(1/q_g)_{PSSU}$ = 5.9819x10^{-5} day/Mscf
$[t *(1/q_g)']_{PSSU}$ = 3.5429x10^{-5} day/Mscf
$(t)_{LPSSUi}$ = 168.0775 hr

Permeability and reservoir length are estimated from the linear flow regime by means of Equations (19) and (20),

$$k^0 = \frac{4144.95\ (9.039323549\ \text{hr})}{(0.052)\ (0.018\ \text{cp})\ (\ 1.85\text{x}10^{-4}\ \text{psi}^{-1})} \left\{ \frac{633.5\ ^\circ\text{R}}{(2)(400\text{ft})\left[(5.15\text{x}10^8)-(2.08\text{x}10^7)\right]\frac{\text{psi}^2}{\text{cp}}(600\ \text{ft})(5.53746\text{x}10^{-6}\frac{\text{dia}}{\text{Mscf}})} \right\}^2 = 0.0503\ \text{md}$$

$$x_e = \frac{64.38\ (633.5\ ^\circ\text{R})\sqrt{9.0303\ \text{hr}}}{2\ (400\text{ft})\left[(5.15\text{x}10^8)-(2.08\text{x}10^7)\right]\frac{\text{psi}^2}{\text{cp}}(5.538\text{x}10^{-6}\frac{\text{dia}}{\text{Mscf}})\ (0.05\ \text{md}\ (0.052)\ (0.018\ \text{cp})(1.85\text{x}10^{-4}\ \frac{1}{\text{psi}}))^{1/2}}$$

x_e = 601.621 ft

The above value of x_e is used in Equation (14) to find the fracture length, x_f,

$$x_f = \frac{601.621\ \text{ft}}{2} = 300.81\ \text{ft}$$

The initial damage is calculated using Equation (21),

$$s_{inicial} = \frac{(2)(0.05)(400)\left[(5.15\text{x}10^8 - 2.08\text{x}10^7\right]}{1424(633.5)}\left(1.1134\text{x}10^{-5}\right)$$

$$s_{inicial} = 0.244$$

Equation (32) applied on the pseudosteady state period is used to calculate the reservoir length.

$$x_e = \frac{\frac{57}{25}\pi * 0.0002637 * 1424 * 633.5\ ^\circ\text{R}}{2\ (0.052)\ (400\ \text{ft})\ (0.018\ \text{cp})\ (1.85\text{x}10^{-4}\ \frac{1}{\text{psi}})\ (300\ \text{ft})\left[(5.15\text{x}10^8)-(2.08\text{x}10^7)\right]\frac{\text{psi}^2}{\text{cp}}(3.5429\text{x}10^{-5})\frac{\text{dia}}{\text{Mscf}}}\frac{252.80178\ \text{hr}}{}$$

$$x_e = 592.323\ \text{ft}$$

Which also leads to produce a value of 299.16 ft for the fracture length by using Equation (14).

Finally, Equation (39) uses the intersection point of the late pseudosteady-state and linear lines, t_{LPSSUi}, to allow obtaining the initial permeability,

$$k^0 = \left[\frac{23.9225(300)\left[(0.052)(0.018)(1.85\times10^{-4})\right]^{0.5}}{(168.075)^{0.5}} \right]^2 = 0.053\ \text{md}$$

4.2. Example-2: Linear model

It is required to find permeability, reservoir length and fracture length from the data reported in Figure-11 and the information given in table 2.

Solution. For the application of the governing equations of each flow in this example, the following data are read from Figure-11,

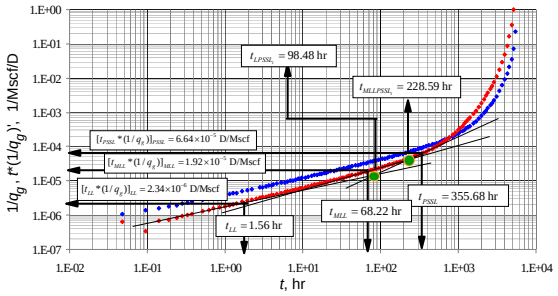

Figure-11. Log-log plot of the reciprocal rate and the reciprocal rate derivative vs. time for the linear synthetic example.

$(t)_{LL}$ = 1.56021 hr
$(1/q_g)_{LL}$ = 4.7468x10^{-6} day/Mscf
$[t*(1/q_g)']_{LL}$ = 2.34379x10^{-6} day/Mscf
$(t)_{MLL}$ = 68.2239 hr
$(1/q_g)_{MLL}$ = 3.4161x10^{-5} day/Mscf
$[t*(1/q_g)']_{MLL}$ = 1.92435x10^{-5} day/Mscf
$(t)_{PSSL}$ = 355.6813 hr
$(1/q_g)_{PSSL}$ = 9.4474x10^{-5} day/Mscf
$[t*(1/q_g)']_{PSSL}$ = 6.64326x10^{-5} day/Mscf
$(t)_{LPSSLi}$ = 98.4825 hr
$(t)_{LPSSLi}$ = 228.5948 hr

Equation (19) applied on the linear flow regime is ideal for calculating the maximum induced permeability which resulted to be 0.048 md. Then, Equation (20) allows calculating a x_e value of 590.8367 ft which used in Equation (14) gives a value of fracture length of 295.4183 ft. An initial skin factor of 0.1042 is found with Equation (21).

Taking advantage of the presence of the multilinear flow regime, permeability 0.034 md representing the transition period mentioned by Fuentes-Cruz *et al.* (2014) is obtained from Equation (23). The estimated geometrical skin factor using Equation (25) for this flow regime resulted to be 0.052.

The pseudosteady state regime is used along with Equation (34) provides a value x_e of 597.2 ft and the points of intersection used in Equation (40) provides the maximum permeability with a value 0.05, while Equation (43) provides minimum induced permeability values of 0.0298 md.

4.3. Example-3: Exponential model

Figure-12 presents synthetic reciprocal rate and reciprocal rate derivative versus time data for an exponential model simulated using information from Table-2. It is required to properly characterize the reservoir by transient-rate interpretation analysis.

Solution. The following information was read from Figure-12.

$(t)_{LE}$ = 0.33095 hr
$(1/q_g)_{LE}$ = 2.3135x10^{-6} day/Mscf
$[t*(1/q_g)']_{LE}$ = 1.06623x10^{-6} day/Mscf
$(t)_{MLE}$ = 7.89562 hr
$(1/q_g)_{MLE}$ = 1.20184x10^{-5} day/Mscf
$[t*(1/q_g)']_{MLL}$ = 6.85377x10^{-6} day/Mscf
$(t)_{PSSE}$ = 845.87182 hr
$(1/q_g)_{PSSE}$ = 3.07091x10^{-4} day/Mscf
$[t*(1/q_g)']_{PSSE}$ = 2.60214x10^{-4} day/Mscf
$(t)_{LPSSEi}$ = 35.69578 hr
$(t)_{LPSSEi}$ = 270.9569 hr

Equation (19) applied on the linear flow regime is very useful for calculating the maximum induced permeability which resulted to be 0.0497 md. Equation (20) provides a x_e value of 598.18 ft which is further used in Equation (14) to find x_f = 299.081 ft. Also from this flow regime an initial skin factor of 0.0507 was found with Equation (21).

The multilinear flow regime is also used to estimate a transition permeability value of 0.0244 md by means of Equation (27). The estimated geometrical skin factor using Equation (29) for this flow regime resulted to be 0.012.

Equation (36) applied on the pseudosteady state regime provides a x_e value of 597.2063 ft and the intersection points used in Equations (45) provides the maximum permeability with a value 0.051, while Equation (47) provides minimum induced permeability values of 0.155 md.

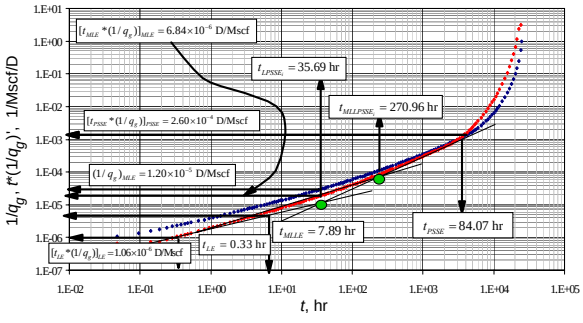

Figure-12. Log-log plot of the reciprocal rate and the reciprocal rate derivative vs. time for the exponential synthetic example.

Table-3. Fluid, reservoir and well information for Example-4.

Parameter	Value	Parameter	Value
h (ft)	306	μ_g (cp)	0.018
ϕ (%)	4.8	x_e (ft)	800
T (°R)	633.5	P_i (psi)	3115
B_{gi} (rb/Mscf)	0.916	P_{wf} (psi)	500
$m(P_i)$ (psi^2/cp)	6.83x10^8	c_t (psi^{-1})	2.51x10^{-4}
$m(P_{wf})$ (psi^2/cp)	2.08x10^7	y (ft)	552
k^0 (md)	2.8x10^{-3}	n_f	3

4.4. Field example: Exponential case

Table-14 contains reservoir, fluid and well properties for a field case presented and solved by Fuentes-Cruz *et al*. (2014) using rate-decline analysis. The rate-time data are reported in Figure-13 and. It is required to find permeability, damage and reservoir length by transient-rate analysis.

It is important to remark that original rate versus time data were not available so they were digitized from the work of Fuentes-Cruz *et al*. (2014). The reciprocal rate derivative was estimated, afterwards.

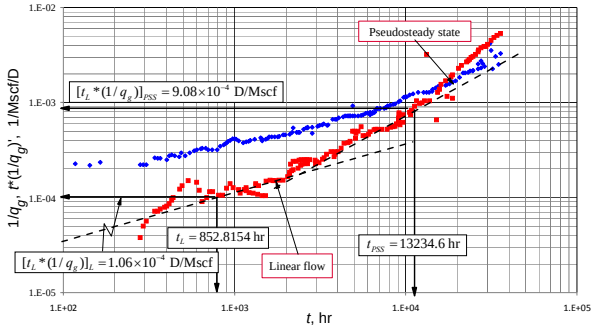

Figure-13. Log-log plot of the reciprocal rate and the reciprocal rate derivative vs. time for the exponential field example.

Solution. The following parameters were read from Figure-13.

$(t)_{LE}$ = 852.8151 hr
$[t*(1/q_g)']_{LE}$ = 1.06x10^{-4} dia/Mscf
$(t)_{PSSE}$ = 13234.6 hr
$[t*(1/q_g)']_{PSSE}$ =9.08x10^{-4} dia/Mscf
$(t)_{LPSSUi}$ = 35.6958 hr

Equation (36), applied on the pseudosteady state regime, is used to calculate a x_e value of 755.58 ft. Now, the use of Equation (19) on the linear flow regime allows finding a maximum induced permeability value of 2.4837x10^{-3} md and Equation (21) provided a damage of 0.346. Table 4 summarizes the results compared to the original work of Fuentes-Cruz *et al*. (2014). Notice that in spite of that the data were digitized the results match well.

Table-4. Results for Example-4 against original results.

Parameter	Fuentes-Cruz *et al.* (2014)	This work	% Error
k° (md)	2.8x10^{-3}	2.48x10^{-3}	11.43
k^*(md)	3.9x10^{-5}	-	
x_e (ft)	800	755.58	5.56
s	0.31	0.346	11.6

5. COMMENTS ON THE RESULTS

The worked examples show the great agreement obtained for all the estimated parameters compared to the values used for the simulation. As far as the field example is concerned, comparing to the output values given by Fuentes-Cruz *et al*. (2014), the results from the equations developed in this work do not match quite well. This is due to be caused by not having the original rate-time data.

6. CONCLUSIONS

a) Several expressions based upon the uniform, linear and exponential flow models introduced by Fuentes-Cruz *et al*. (2014) for the estimation of permeability, skin factor, fracture length and lateral reservoir length in ultralow reservoirs by transient-rate analysis using the *TDS* technique were presented and successfully tested with synthetic and field examples.

b) It is presented the characterization of a new feature behavior taking place between the linear flow regime and the pseudosteady state period was found to be represented by a slope of either 0.66 (exponential model) or 0.61 (linear model) on the reciprocal rate derivative. A combination of linear flow regimes was assumed to take place. Then, this behavior was arbitrarily named called "multilinear flow regime". However, a simulation study is recommended to properly identify this flow behavior.

ACKNOWLEDGEMENTS

The authors gratefully thank the Most Holy Trinity and the Virgin Mary mother of God for all the blessing received during their lives.

Nomenclature

B_g	Volumetric factor, rb/Mscf
c_t	System total compressibility, 1/psi
k^0	Maximum permeability induced, md
k^*	Minimum permeability induced, md
$m(P)$	Pseudopressure, psi^2/cp
n_f	Number of main hydraulic-fracture planes
P	Pressure, psi
$\bar{P}$	Laplace-space pressure
P_{wf}	Bottomhole flowing pressure, psi
$\bar{q}$	Laplace-space flow rate
$1/q$	Reciprocal flowrate , D/Mscf
$t*(1/q)'$	Reciprocal flow rate derivative, D/Mscf
s	Skin factor

t	Time, hr
T	Absolute temperature, °R
u	Laplace space variable
x_e	effective reservoir width, ft
x_f	Hydraulic fracture half-length, ft
y^*	half-length of stimulated reservoirs volume element, ft

Greeks

ϕ	Porosity, fraction
μ	Viscosity, cp

Suffices

g	Gas
i	Initial
BDS	Boundary-dominated state
D	Dimensionless
DA	Dimensionless based on drainage area
PSS	Pseudosteady state
sc	Standard conditions
ST	Short times
LU	Linear flow, uniform model
LL	Linear flow, linear model
LE	Linear flow, exponential model
MLL	Multilinear
$MLLU$	Multilinear flow, uniform model
$MLLL$	Multilinear flow, linear model
$MLLE$	Multilinear flow, exponential model
$PSSU$	Pseudosteady state, uniform model
$PSSL$	Pseudosteady state, linear model
$PSSE$	Pseudosteady state, exponential model
$LPSSUi$	Intersection point between linear flow and pseudosteady state, uniform model
$LPSSLi$	Intersection point between linear flow and pseudosteady state, lineal model
$LPSSEi$	Intersection point between linear flow and pseudosteady state, exponential model
$MLLPSSLi$	Intersection point between multlinear flow and pseudosteady state, linear model
$MLLPSSEi$	Intersection point between multlinear flow and pseudosteady state, exponential model

APPENDIX-A: GOVERNING EQUATIONS FOR OIL FLOW

A.1. Linear flow regime

The dimensionless equation representing the linear flow is independent of the model and the variation of permeability, the behavior is given by:

$$t_{DL}*(1/q_D)'_L = \frac{1}{2}\pi^{\frac{3}{2}}\sqrt{t_D} \quad (A.1)$$

Once the dimensionless terms given by Equations (5) and (12) are plugged into Equation (A.1), the lateral extent of the stimulated reservoir volume can be solved for:

$$x_e = \frac{12.77\mu B}{n_f k^{0.5} h\left[P_i - P_{wf}\right]\left[t*(1/q)'_L\right]}\left[\frac{t_L}{(\phi\mu c_t)}\right]^{0.5} \quad (A.2)$$

From the above equation it is possible to know the value of permeability:

$$k = \left[\frac{12.77\mu B}{n_f x_e h\left[P_i - P_{wf}\right]\left[t*(1/q)'_L\right]}\left[\frac{t_L}{(\phi\mu c_t)}\right]^{0.5}\right]^2 \quad (A.3)$$

A.2. Multilinear flow regime

A.2.1. Linear model

The general equation describing this flow regime, for the linear model in dimensionless terms is:

$$t_D*(1/q_D)'_{MLL} = \frac{250}{50}(t_D)^{0.6135}_{MLL} \quad (22)$$

It is possible to obtain from Equation (A.4) equations for calculating k and x_e, respectively,

$$k = \left\{\frac{4.4(t_{MLL})^{0.6135}}{(\phi\mu c_{ti})^{0.6135} x_e^{1.227} n_f h\left[P_i - P_{wf}\right]\left[t*(1/q)'_{MLL}\right]}\right\}^{\frac{1}{0.3865}} \quad (A.4)$$

$$x_e = \left\{\frac{4.4(t_{MLL})^{0.6135}}{(\phi\mu c_{ti})^{0.6135} k^{0.3865} n_f h\left[P_i - P_{wf}\right]\left[t*(1/q)'_{MLL}\right]}\right\}^{\frac{1}{1.227}} \quad (A.5)$$

The geometrical skin damage equation obtained from the multilinear flow:

$$s_{MLL} = 4.8903(t_D)^{0.6135}_{MLL}\left[\frac{(1/q_D)_{MLL}}{t_D*(1/q)'_{MLL}} - 1.629991\right] \quad (A.6)$$

A.2.2. Exponential model

The general dimensionless equation which describes the behavior of linear flow in the exponential model is:

$$t_D*(1/q_D)'_{MLE} = \frac{405}{50}(t_D)^{0.6612}_{MLE} \quad (26)$$

After replacing Equations (5) and (12) into Equation (26) and solving for both k and x_e gives:

$$k = \left\{\frac{4.9(t_{MLE})^{0.6612}}{(\phi\mu c_{ti} x)^{0.6612} x_e^{1.3224} n_f h\left[m(P_i) - m(P_{wf})\right]\left[t*(1/q)'_{MLE}\right]}\right\}^{\frac{1}{0.3388}} \quad (A.7)$$

$$x_e = \left\{ \frac{4.9(t_{MLE})^{0.6612}}{(\phi\mu c_{ti}x)^{0.6612} k^{0.3388} n_f h \left[m(P_i) - m(P_{wf}) \right] \left[t*(1/q)'_{MLE} \right]} \right\}^{\frac{1}{1.3224}} \quad \text{(A.8)}$$

The developed equation for calculating the geometrical kin factor, for exponential induced permeability model is,

$$s_{MLE} = 0.03488 \left(\frac{kt_{MLE}}{\phi\mu c_i x_e^{\,2}} \right)^{0.6612} \left[\frac{(1/q)_{MLE}}{t*(1/q)'_{MLE}} - 1.512402 \right] \quad \text{(A.9)}$$

A.3. Pseudosteady state period

A.3.1. Uniform model

After replacing Equations (5) and (12) in Equation (31) and solving the reservoir length,

$$x_e = \frac{0.267}{n_f \phi h (\mu c_t)_i \, y \left[P_i - P_{wf} \right]} \frac{t_{PSSU}}{\left[t*(1/q)' \right]_{PSSU}} \quad \text{(A.10)}$$

A.3.1. Linear model

Same as above for Equation (33) yields,

$$x_e = \frac{0.358}{n_f h \phi (\mu c_t)_i \, y \left[P_i - P_{wf} \right]} \frac{t_{PSSL}}{\left[t*(1/q)' \right]_{PSSL}} \quad \text{(A.11)}$$

A.3.1. Exponential model

The replacement of Equations (5) and (12) in Equation (35) leads to solve for the reservoir length,

$$x_e = \frac{0.596}{n_f h \phi (\mu c_t)_i \, y \left[m(P_i) - m(P_{pwf}) \right]} \frac{t_{PSSE}}{\left[t*(1/q)' \right]_{PSSE}} \quad \text{(A.12)}$$

REFERENCES

El-Banbi A., H. and Wattenbarger R.A. 1998. Analysis of Linear Flow in Gas Well Production. Paper SPE 39972 presented at the SPE Gas Technology Symposium, Calgary, Alberta, Canada.

Escobar F.H., Sanchez J.A. and Cantillo J.H. 2008. Rate Transient Analysis for Homogeneous and Heterogeneous Gas Reservoirs using The *TDS* Technique. CT and F - Ciencia, Tecnología y Futuro. 4(4): 45-59. ISSN 0122-5383.

Escobar F.H., Rojas M.M. and Bonilla L.F. 2012. Transient-Rate Analysis for Long Homogeneous and Naturally Fractured Reservoir by the *TDS* Technique. Journal of Engineering and Applied Sciences. ISSN 1819-6608. 7(3): 353-370.

Escobar F.H., Rojas M.M. and Cantillo J.H. 2012. Straight-Line Conventional Transient Rate Analysis for Long Homogeneous and Heterogeneous Reservoirs. Dyna. Year 79, Nro. 172, pp. 153-163. ISSN 0012-7353. April.

Escobar F.H., Castro J.A. and Mosquera J.S. 2014. Rate-Transient Analysis for Hydraulically Fractured Vertical Oil and Gas Wells. Sent to Journal of Engineering and Applied Sciences requested for publication.

Escobar F.H., Alzate H.D. and Moreno L. 2013. Effect of Extending the Radial Superposition Function to Other Flow Regimes. Journal of Engineering and Applied Sciences. 8(8): 625-634.

Fuentes-Cruz G., Gildin E. and Valko P. 2014. Analyzing Production Data from Hydraulically Fractured Wells: the Concept of Induced Permeability Field. SPE Formation Evaluation. pp. 1-13.

Ge J. and Ghassemi A. 2011. Permeability Enhancement in Shale Gas Reservoirs after Stimulation by Hydraulic Fracturing. Paper AR11-514 presented at the Rock Mechanics / Geomechanics Symposium, San Francisco, CA.

Montenegro-G. L.M. and Bernal-V. K.M. 2014. Análisis del Comportamiento del Recíproco del Caudal y su Derivada en Función de Tiempo Adimensional en Yacimientos no Convencionales de Hidrocarburos - Gas Shale. B.Sc. Thesis. Universidad Surcolombiana. Neiva (Huila-Colombia). June.

Palmer I.D., Moschovidis Z.A. and Cameron J.R. 2007. Modeling Shear Failure and Stimulation of the Barnett Shale after Hydraulic Fracturing. Paper SPE 106113 presented at the SPE Hydraulic Fracturing Technology Conference, College Station, Texas, U.S.A.

Tiab D. 1993. Analysis of Pressure and Pressure Derivative without Type-Curve Matching: 1- Skin and Wellbore Storage. Journal of Petroleum Science and Engineering. 12: 171-181.

Wattenbarger R.A., El-Banbi A.H., Villegas M.E. and Maggard J. B. 1998. Production Analysis of Linear Flow into Fractured Tight Gas Wells. Paper SPE 39931 presented at the SPE Rocky Mountain Regional/Low Permeability Reservoirs Symposium, Denver, Colorado.